A New Iterative Method for Passive Doppler Geolocation Based on Semi-Definite Programming

Mustafa Atahan Nuhoglu* † Yasar Kemal Alp* Aydin Bayri* Hakan Ali Cirpan†

* Radar Electronic Warfare and Intelligence Systems Division, ASELSAN A.S., Ankara, Turkey
† Electical and Electronics Engineering Department, Istanbul Technical University, Istanbul, Turkey
{manuhoglu, ykalp, bayri}@aselsan.com.tr, hakan.cirpan@itu.edu.tr

***Abstract*—In this work, we propose a new iterative method running on a receiver located at a moving platform for uncooperative radar geolocation. The method uses Doppler-shifted measurements of the stationary radar signals due to the platform motion. The carrier frequency and the position of the radar are estimated jointly in each iteration by solving a semi-definite program. Conducted experiments show that a few iterations are enough for convergence to stable estimates. Hence, the proposed method has a significant computational advantage compared to traditional techniques, which require an extensive grid search on either position or carrier frequency parameter space.**

***Index Terms*—Emitter geolocation, semi-definite programming, Doppler-shifted frequency, computational complexity**

I. Introduction

Passive emitter geolocation using Doppler-shifted frequency measurements has been utilized in many application areas including radar and sonar systems, satellite navigation, research and rescue missions [1]–[13]. If the carrier frequency of the signals emitted by the radar is known, as in the case of SARSAT/CORPAS systems, there are iterative and algebraic methods which follow Point of Closest Approach (PCA) [1], [2]. Similarly, the Direct Position Determination (DDP) method, which is used in both narrowband and wideband signal geolocation, successfully estimates target position even in low SNR (signal-to-noise ratio) scenarios, provided that the carrier frequency is known beforehand [3], [4].

If the carrier frequency is unknown, the problem is more complex and solution methods are based on extensive grid search. These methods can be divided into two classes depending on the measurement type. In the first class, there are methods using frequency measurements. They perform a grid search on either position or carrier frequency parameter space for geolocation [6], [12]. The methods in the second class use frequency change of rate (FCR) measurements. Their performance is highly sensitive to the platform trajectory since frequency line trackers, which produce FCR measurements, require a constant relative speed between the receiver and the emitter to provide reliable outputs [5]. Furthermore, they also utilize a grid search procedure on position parameter space [5], [6]. Therefore, all of these methods suffer from high computational complexity.

The Doppler geolocation problem is non-linear and non-convex whether the carrier frequency is known or not. In order to transform it to a convex program by applying convex relaxation methodology, there have been proposed several semi-definite programming (SDP) based approaches [7]–[11]. However, all of these methods either assume that the carrier frequency is known or they additionally require Time Difference of Arrival measurements.

To the best of our knowledge, there exists no work regarding relaxation of uncooperative radar geolocation without knowledge of its carrier frequency, when only Doppler-shifted frequency measurements are available. To fill this gap and to overcome the aforementioned computational complexity burden encountered in the grid search methods, we propose a new iterative SDP relaxation method, which jointly solves carrier frequency and position in each iteration. The extended simulations show that the proposed technique provides stable estimates in only a few iterations.

The paper is organized as follows: Section II describes the signal model. Section III explains the proposed method. Section IV demonstrates the simulation results and the last section is spared for conclusions. Throughout the paper, uppercase and lowercase bold letters denote matrices and vectors, respectively. The symbols $\|\cdot\|$ and $\mathrm{Tr}(\cdot)$ denote the Frobenius norm and trace. $\mathbf{X} \succcurlyeq 0$ means matrix $\mathbf{X}$ is positive semi-definite. $\hat{\mathbf{x}}$ denotes the estimate of $\mathbf{x}$. x_i will denote the i-th entry of vector $\mathbf{x}$. Similarly, $X_{i,j}$ will denote the i-th row and j-th column of matrix $\mathbf{X}$, while $\mathbf{X}_{i:j,k:l}$ denotes the submatrix of $\mathbf{X}$ formed by rows i to j and columns k to l.

II. Signal Model

Since the receiver is located on a moving platform, due to the Doppler effect, the frequency of the received radar signal is given by:

$$\tilde{f}_i = f_0\left(1 + \frac{\|\mathbf{v}_i\| \cos\alpha_i}{c}\right) + \xi_i \ . \tag{1}$$

Here i is the time index, $\tilde{f}_i$ is the received signal frequency, f_0 is the carrier frequency of the radar, $\mathbf{v}_i$ is the receiver velocity vector, c is the speed of light and $\cos\alpha_i$ is the cosine of the angle between the receiver velocity vector and range vector. ξ_i denotes noise observed at the receiver and it is assumed to be additive white Gaussian (AWGN) with zero mean and σ^2 variance.

Fig. 1 demonstrates the angle α. $d_{i,i-1}$ is the distance between two sequential positions of the platform, at time

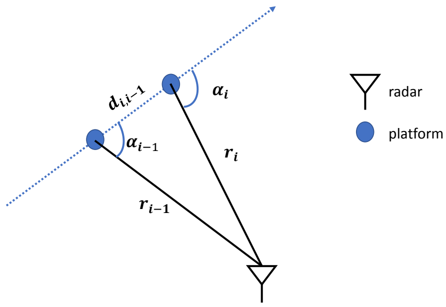

Fig. 1: Visualization of α for two sequential samples. Triangle is the radar, circles are the sequential positions of the platform and the arrowhead indicates the direction of the receiver movement. d is the distance between two positions of the receiver, while r is the distance between the receiver and the radar.

instants i and $i-1$, of the receiver, where r_i is the distance between the radar and the receiver. $\cos\alpha_i$ is given by:

$$\cos\alpha_i = \frac{\mathbf{v_i}^T(\mathbf{x}-\mathbf{p}_i)}{\|\mathbf{v}_i\| r_i}, \tag{2}$$

where $\mathbf{p}_i = [p_i^x, p_i^y]^T$ is the receiver position, $\mathbf{x} = [x, y]^T$ is the radar position to be estimated and $r_i = \|\mathbf{x}-\mathbf{p}_i\|$ is the distance of the receiver to the radar. The equation in (1) can also be written as:

$$\tilde{f}_i = f_0(1 + \frac{\mathbf{v_i}^T(\mathbf{x}-\mathbf{p}_i)}{cr_i}) + \xi_i \ . \tag{3}$$

The Maximum Likelihood (ML) cost function defined as

$$d(f_0, \mathbf{x}) = \sum_{i=1}^{N} \frac{1}{\sigma_i^2}(\tilde{f}_i - f_0(1 + \frac{\mathbf{v_i}^T(\mathbf{x}-\mathbf{p}_i)}{cr_i}))^2 \tag{4}$$

is to be minimized over $\mathbf{x} \in \mathbb{R}^2$ and $f_0 \in \mathbb{R}$.

III. Proposed Method

The ML cost function in (4) is non-convex in $\mathbf{x}$. In order to first turn it into a Constrained Weighted Least Squares (CWLS) problem, we utilize sine law on the triangle shown in Fig. 1:

$$\frac{d_{i,i-1}}{\sin(\alpha_i - \alpha_{i-1})} = \frac{r_i}{\sin\alpha_{i-1}} \ . \tag{5}$$

Then leaving r_i alone:

$$r_i = \frac{d_{i,i-1}\sin\alpha_{i-1}}{\sin(\alpha_i - \alpha_{i-1})} = \frac{d_{i,i-1}\sin\alpha_{i-1}}{\sin\alpha_i\cos\alpha_{i-1} - \sin\alpha_{i-1}\cos\alpha_i} \ . \tag{6}$$

Exact $\sin\alpha$ and $\cos\alpha$ values can be found by (2). However, $\mathbf{x}$ is unknown. Therefore, the receiver can approximate $\sin\alpha$ and $\cos\alpha$ values only from its frequency measurements. The following estimates can be derived from (1):

$$\hat{\cos}\alpha_i = (\frac{\tilde{f}_i}{f_0} - 1)\frac{c}{\|\mathbf{v}_i\|}, \tag{7}$$

$$\hat{\sin}\alpha_i = \pm\sqrt{1 - (\frac{\tilde{f}_i}{f_0} - 1)^2 \frac{c^2}{\|\mathbf{v}_i\|^2}} \ . \tag{8}$$

Notice that sign of $\sin\alpha_i$ is unimportant since both the numerator and denominator in (6) have $\sin\alpha_i$ terms. In our scenario, it is chosen as positive. By using (7-8), (6) can be written as:

$$r_i = \frac{\theta}{\gamma - \phi} \tag{9}$$

where

$$\theta = d_{i,i-1}\sqrt{1 - (\frac{\tilde{f}_{i-1}}{f_0} - 1)^2 \frac{c^2}{\|\mathbf{v}_{i-1}\|^2}}, \tag{10}$$

$$\gamma = \sqrt{1 - (\frac{\tilde{f}_i}{f_0} - 1)^2 \frac{c^2}{\|\mathbf{v}_i\|^2}}(\frac{\tilde{f}_{i-1}}{f_0} - 1)\frac{c}{\|\mathbf{v}_{i-1}\|}, \tag{11}$$

$$\phi = \sqrt{1 - (\frac{\tilde{f}_{i-1}}{f_0} - 1)^2 \frac{c^2}{\|\mathbf{v}_{i-1}\|^2}}(\frac{\tilde{f}_i}{f_0} - 1)\frac{c}{\|\mathbf{v}_i\|} \ . \tag{12}$$

Then, to linearize r_i in f_0, first order Taylor series expansion around an approximated f_0 is utilized. The approximated carrier frequency ($\hat{f}_0$) value is chosen as a simple mean of the received frequency measurements. After the expansion, r_i can be written as:

$$r_i = a_i + b_i f_0 \ . \tag{13}$$

Substituting (13) in (4) results in the following cost function:

$$h(f_0, \mathbf{x}) = \sum_{i=1}^{N} \frac{1}{\sigma_i^2}\Big(\tilde{f}_i - f_0(1 + \frac{\mathbf{v_i}^T(\mathbf{x}-\mathbf{p}_i)}{c(a_i + b_i f_0)})\Big)^2,$$
$$= \sum_{i=1}^{N} \frac{1}{W_i}\Big(\tilde{f}_i c(a_i + b_i f_0) - f_0 c(a_i + b_i f_0) - f_0 \mathbf{v_i}^T(\mathbf{x}-\mathbf{p}_i)\Big)^2, \tag{14}$$

where

$$W_i = \sigma_i^2 c^2 (a_i + b_i f_0)^2 \ . \tag{15}$$

Rearranging (14) yields:

$$\sum_{i=1}^{N} \frac{1}{W_i}\Big(f_0(\tilde{f}_i c b_i - c a_i + \mathbf{v_i}^T\mathbf{p}_i) + f_0^2(-cb_i) + f_0\mathbf{x}^T(-\mathbf{v_i}) + 1(\tilde{f}_i c a_i)\Big)^2 \ . \tag{16}$$

Minimization of the cost function above can be written as a CWLS problem:

$$\begin{aligned} \min_{\mathbf{x}\in\mathbb{R}^2, f_0\in\mathbb{R}^1} \quad & \mathbf{g}^T\mathbf{D}^T\mathbf{W}^{-1}\mathbf{D}\mathbf{g} \ , \\ \text{s.t.} \quad & g_2 = g_1^2 \ , \\ & g_5 = 1, \end{aligned} \tag{17}$$

where

$$\mathbf{g} = \big[f_0,\ f_0^2,\ f_0\mathbf{x}^T,\ 1\big]^T \ ,$$
$$\mathbf{D} = \begin{bmatrix} k_1, & l_1, & \mathbf{p}_1^T, & s_1 \\ k_2, & l_2, & \mathbf{p}_2^T, & s_2 \\ \vdots & \vdots & \vdots & \vdots \\ k_N, & l_N, & \mathbf{p}_N^T, & s_N \end{bmatrix} ,$$
$$\mathbf{W} = diag(\big[W_1,\ W_2, ...,\ W_N\big]) \ , \tag{18}$$

and entries of D are:

$$\begin{aligned} k_i &= \tilde{f}_i c b_i - c a_i + \mathbf{v_i}^T \mathbf{p}_i \ , \\ l_i &= -c b_i \ , \\ \mathbf{p}_i^T &= -\mathbf{v_i}^T \ , \\ s_i &= \tilde{f}_i a_i c \ . \end{aligned} \tag{19}$$

To relax the problem in (17) into a convex one, the SDP approach is followed. $\mathbf{G} = \mathbf{g}\mathbf{g}^T$ is defined as the variable of the optimization by utilizing the lifting technique given in [14]. Then, (17) can be equivalently written as:

$$\begin{aligned} \min_{\mathbf{G} \in \mathbb{R}^{5x5}} \quad & \mathrm{Tr}(\mathbf{D}^T \mathbf{W}^{-1} \mathbf{D} \mathbf{G}) \\ \text{s.t.} \quad & \mathbf{P} \succcurlyeq 0 \ , \\ & \mathrm{rank}(\mathbf{P}) = 1 \ , \\ & G_{5,5} = 1 \ , \end{aligned} \tag{20}$$

where $\mathbf{P} = \begin{bmatrix} G_{2,2}, & G_{1,1} \\ G_{1,1}, & 1 \end{bmatrix}$.

By dropping the rank constraint above, we relax the problem and turn it into a convex program. Since possible maximum Doppler shift is known by the receiver, linear inequality constraints on the following lower and upper bounds of the carrier frequency are additionally inserted:

$$f_0^{\max} = \frac{\min\limits_i \tilde{f}_i}{1 - \frac{\max\limits_i \|\mathbf{v}_i\|}{c}} \geq f_0 \geq \frac{\max\limits_i \tilde{f}_i}{1 + \frac{\max\limits_i \|\mathbf{v}_i\|}{c}} = f_0^{\min} \ , \tag{21}$$

where $f_0^{\min}$ and $f_0^{\max}$ are the lower and upper bounds for f_0, respectively. Finally, the SDP based optimization problem becomes:

$$\begin{aligned} \min_{\mathbf{G} \in \mathbb{R}^{5x5}} \quad & \mathrm{Tr}(\mathbf{D}^T \mathbf{W}^{-1} \mathbf{D} \mathbf{G}) \\ \text{s.t.} \quad & \mathbf{P} \succcurlyeq 0 \ , \\ & G_{5,5} = 1 \ , \\ & f_0^{\max} \geq G_{1,5} \geq f_0^{\min} \ , \\ & (f_0^{\max})^2 \geq G_{1,1} \geq (f_0^{\min})^2 \ , \\ & (f_0^{\max})^2 \geq G_{2,5} \geq (f_0^{\min})^2 \ , \\ & (f_0^{\max})^3 \geq G_{1,2} \geq (f_0^{\min})^3 \ , \\ & (f_0^{\max})^4 \geq G_{2,2} \geq (f_0^{\min})^4 \ , \end{aligned} \tag{22}$$

which can be optimally solved by interior-point algorithms [15]. If the globally optimal solution $\hat{\mathbf{G}}$ is rank-one, we can decompose $\hat{\mathbf{G}}$ as $\hat{\mathbf{G}} = \hat{\mathbf{g}}\hat{\mathbf{g}}^T$, where $\hat{\mathbf{g}}$ is the optimal solution of (17). If $\hat{\mathbf{G}}$ is not rank-one, we can utilize singular value decomposition (SVD) to $\hat{\mathbf{G}}$ [14]:

$$\hat{\mathbf{G}} = \sum_{i=1}^{5} \lambda_i \mathbf{u_i} \mathbf{u_i}^T \tag{23}$$

where $\lambda_1 \geq \lambda_2 \geq \ldots \geq \lambda_5$ are the singular values and $\mathbf{u}_1, \ldots, \mathbf{u}_5 \in \mathbb{R}^5$ are the corresponding singular vectors. Then, the best rank-one approximation to $\hat{\mathbf{G}}$ can be constructed as $\mathbf{G}_1 = \lambda_1 \mathbf{u}_1 \mathbf{u}_1^T$. After that, $\hat{\mathbf{g}}$ can be estimated by $\hat{\mathbf{g}} = \sqrt{\lambda_1}\mathbf{u}_1$ and the carrier frequency is found by $\hat{f}_0 = \hat{g}_1$.

Algorithm - I

Input: $\tilde{f}_i$: frequency measurement, $\mathbf{v}_i$: velocity vector of platform, $\mathbf{p}_i$: position vector of receiver $\forall\, i = 1, 2, ..., N$
Output: $\mathbf{x}$: radar position vector, f_0: radar carrier frequency

$j \leftarrow 0$.
$\mathbf{W} \leftarrow \mathbf{I}_N$.
$\hat{f}_0^j \leftarrow \frac{1}{N}\sum_{i=1}^{N} \tilde{f}_i$.
Find a_i and b_i values in (13) using $\hat{f}_0^j$ $\forall\, i = 1, 2, ..., N$.
Construct $\mathbf{D}$ using (19).
Find $\hat{\mathbf{G}}^j$ by solving (22).
Apply SVD to $\hat{\mathbf{G}}^j$ and find its singular values $\lambda_1^j \geq \lambda_2^j \geq \ldots \geq \lambda_5^j$ and the corresponding left singular vectors $\mathbf{u}_1^j, \mathbf{u}_2^j, \ldots, \mathbf{u}_5^j$.
$\hat{\mathbf{g}}^j \leftarrow \sqrt{\lambda_1^j}\mathbf{u}_1^j$.
Update $\hat{f}_0$: $\hat{f}_0^{j+1} \leftarrow \hat{g}_1$.
Compute q^j using (25).
while $q^j \geq F$ and $j < N_{iter}$ **do**
    Recalculate a_i and b_i values in (13) using $\hat{f}_0^{j+1}$ $\forall\, i = 1, 2, ..., N$.
    Update $\mathbf{W}$ using $\hat{f}_0^{j+1}$ in (24).
    Construct $\mathbf{D}$ using (19).
    Find $\hat{\mathbf{G}}^{j+1}$ by solving (22).
    Apply SVD to $\hat{\mathbf{G}}^{j+1}$ and find its singular values: $\lambda_1^{j+1} \geq \lambda_2^{j+1} \geq \ldots \geq \lambda_5^{j+1}$ and the corresponding left singular vectors: $\mathbf{u}_1^{j+1}, \mathbf{u}_2^{j+1}, \ldots, \mathbf{u}_5^{j+1}$.
    $\hat{\mathbf{g}}^{j+1} \leftarrow \sqrt{\lambda_1^{j+1}}\mathbf{u}_1^{j+1}$.
    $j \leftarrow j + 1$.
    Update f_0: $\hat{f}_0^{j+1} \leftarrow \hat{g}_1^j$.
    Compute q^j using (25).
end while
Estimate the radar position: $\mathbf{x} \leftarrow \hat{\mathbf{g}}_{3:4}^j / \hat{g}_1^j$.
Estimate the radar carrier frequency: $f_0 \leftarrow \hat{g}_1^j$.

The manual update is utilized by recalculating (13) using $\hat{f}_0$ and recomputing a_i, b_i values. Notice that, weighting matrix $\mathbf{W}$ is initially not known as it requires knowledge of f_0 and it is not updated during the optimization process. Hence, it is initialized as an identity matrix and manually updated as the following:

$$W_{i,i} = \sigma_i^2 c^2 (a_i + b_i \hat{f}_0)^2 \ . \tag{24}$$

Then, (22) is resolved. This procedure is iteratively repeated. The iterations are terminated when the maximum number of iterations is reached or the change of $\hat{f}_0$ between two consecutive iterations

$$q^j = \|\hat{f}_0^j - \hat{f}_0^{j-1}\|, \tag{25}$$

drops under a custom threshold. In (25), j denotes the iteration number. Once the iterations are terminated, the radar position is given by $\hat{\mathbf{g}}_{3:4}/\hat{g}_1$. This procedure is summarized in Algorithm - I.

IV. Results and Analysis

Results in Fig. 4, 5, 6 are taken according to the scenario in Fig. 2 when the carrier frequency of the radar is 1 GHz,

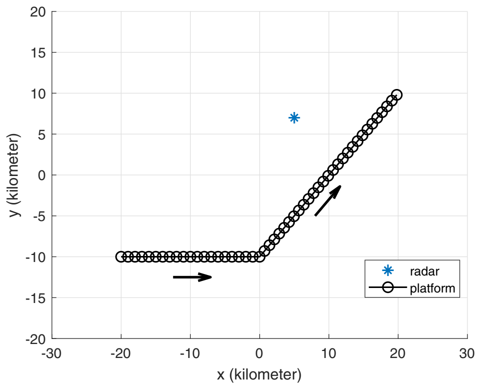

Fig. 2: Platform-radar geometry: the arrows indicate direction of platform movement.

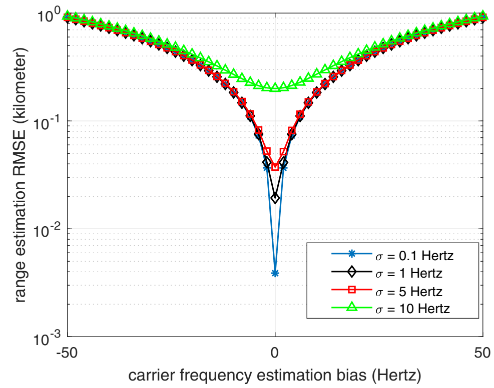

Fig. 3: Range estimation RMSE (kilometer) versus carrier frequency bias (Hertz). Results are taken according to the scenario in Fig. 2.

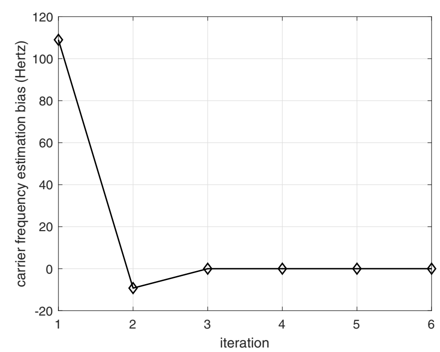

Fig. 4: Carrier frequency estimation bias (Hertz) versus iteration.

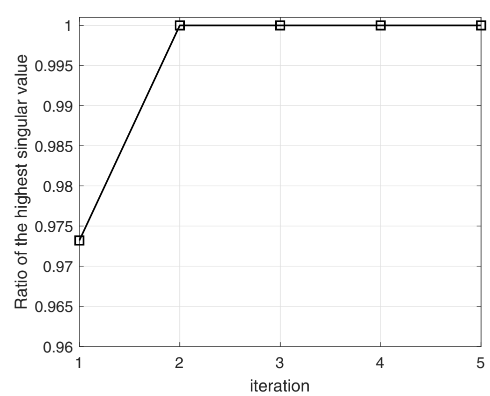

Fig. 5: Ratio of the highest singular value of $\hat{\mathbf{G}}^j$ versus iteration.

speed of the platform carrying the receiver is 100 m/s and standard deviation of the frequency measurement error is $\sigma = 1$ Hz. A single platform would yield ambiguity if it does not maneuver. However, in our scenario, it maneuvers once. Hence there appears no ambiguity. Moreover, the SDP solver, SDPT3, of the convex optimization tool CVX [16], [17] is preferred to obtain the solutions to the relaxed SDP problem.

To demonstrate the effectiveness of the manual steps, Fig. 3 analyzes the performance of linearization operation on r_i by the expansion in (13). In Fig. 3, range estimation RMSE (Root Mean Square Error) against carrier frequency estimation bias for different noise levels is demonstrated. The bias is given by $bias = \hat{f}_0 - f_0$ and the range estimation RMSE is defined as:

$$RMSE = \sqrt{\frac{1}{NM}\sum_{j=1}^{M}\sum_{i=1}^{N}(\hat{r}_{i,j} - r_{i,j})^2} \tag{26}$$

where $\hat{r}_{i,j} = a_{i,j} + b_{i,j}(f_0 + bias)$ is the estimated range, $r_{i,j} = \|\mathbf{x} - \mathbf{p}_{i,j}\|$ is the true range, i is the sample index, N is total number of samples and j is the independent run index, where $M = 500$ is total number of the runs. It is observed that the carrier frequency estimation bias becomes more dominant when the noise level is low. For higher noise levels, the range estimation performance becomes less dependent on the carrier frequency estimation bias. The proposed method aims to provide better range estimates by decreasing $bias$ at each iteration.

The bias of the carrier frequency estimation error as a function of iteration number is given in Fig. 4. The estimated carrier frequency in the first iteration is the mean of frequency measurements. Hence, there is high bias at the first iteration. The estimated carrier frequency converges to the true value in the third iteration. This shows that $\hat{\mathbf{G}}^3$, which is the solution of (22) in the third iteration, is rank-one, therefore, $\hat{\mathbf{g}}^3$ is successfully recovered.

As indicated after (22), if $\hat{\mathbf{G}}^j$ is not rank-one, it results in inaccurate $\hat{\mathbf{g}}^j$ recovery. To investigate the rank properties of $\hat{\mathbf{G}}$, the ratio of the highest singular value to the sum of all singular values as a function of iteration number is analyzed in Fig. 5. This ratio is defined as:

$$singularRatio^j = \frac{\lambda_1^j}{\sum_{i=1}^{5}\lambda_i^j} \tag{27}$$

where j is iteration number and λ_i^j is i-th highest singular value of $\hat{\mathbf{G}}^j$. It can be seen that $singularRatio^1$ is close to one but not exactly, which means that the output of the method at the first iteration is almost rank-one. After the third iteration, this ratio becomes one. Hence, manual updates behave like a regularizer, which shape $\hat{\mathbf{G}}$ in a way that it points a single direction in five dimensional space.

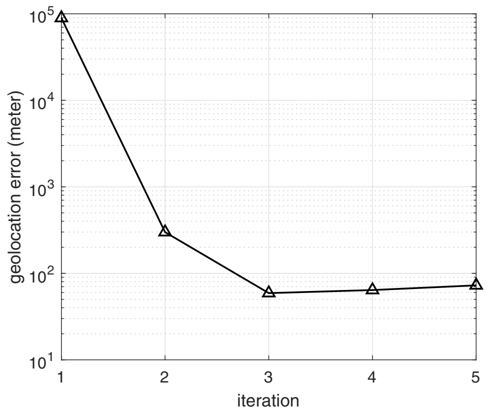

Fig. 6: Geolocation error (meter) versus iteration.

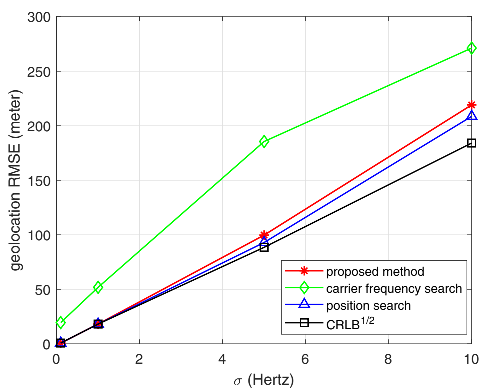

Fig. 7: Geolocation RMSE (meter) versus standard deviation of frequency measurement noise (Hertz).

In Fig. 6, geolocation error against iterations is analyzed. It is formulated as:

$$geoError^j = \|\hat{\mathbf{g}}_{3:4}/\hat{g}_1 - \mathbf{x}\| \ . \tag{28}$$

As observed, the geolocation error drops as the iterations proceed. While the estimated carrier frequency converges to the true value, the range estimation gets better and the estimated radar position gets closer to the true position.

Finally, the proposed method is compared with the grid search methods, which are based on carrier frequency [13] and position [6] in addition to the CRLB [13]. 500 independent runs are utilized for analysis of geolocation RMSE against the frequency measurement noise standard deviation $\sigma \in \{0.1, 1, 5, 10\}$ Hertz, which is shown in Fig. 7. It is seen that the proposed method is able to meet the CRLB at lower noise levels while it still provides accurate position estimates for high noise levels. The proposed method outperforms the method in [13] at all levels of noise. Compared to [6], it performs slightly worse at high noise levels, which is acceptable, since the proposed method provides solutions in only a few iterations instead of utilizing a grid search procedure requiring high computational power.

V. Conclusion

In this work, we propose a new method exploiting SDP relaxation to solve the non-convex optimization problem of uncooperative radar geolocation using only frequency measurements. Geolocation of radars with unknown carrier frequencies is considered and extended simulations are conducted. Results show that the proposed method is able to jointly estimate the radar position and its carrier frequency in only a few iterations. Therefore, it is a computationally inexpensive alternative to the traditional methods requiring extensive grid search procedures. It is also seen that the proposed method meets the CRLB at lower noise levels, while it still provides accurate position estimates for low signal-to-noise ratio scenarios.

References

[1] P. Schmid, F. Vonbun, and J. Lynn, “Single pass doppler positioning for search and rescue satellite missions,” 1976.

[2] N. H. Nguyen and K. Doğançay, “Algebraic solution for stationary emitter geolocation by a leo satellite using doppler frequency measurements,” in *2016 IEEE International Conference on Acoustics, Speech, and Signal Processing (ICASSP)*. IEEE, 2016, pp. 3341–3345.

[3] A. Amar and A. J. Weiss, “Localization of narrowband radio emitters based on doppler frequency shifts,” *IEEE Transactions on Signal Processing*, vol. 56, no. 11, pp. 5500–5508, 2008.

[4] D. Wang and Y. Wu, “Statistical performance analysis of direct position determination method based on doppler shifts in presence of model errors,” *Multidimensional Systems and Signal Processing*, vol. 28, no. 1, pp. 149–182, 2017.

[5] Y. Chan, “A 1-d search solution for localization from frequency measurements,” *IEEE journal of oceanic engineering*, no. 3, pp. 431–437, 1994.

[6] F. Guo, Y. Fan, Y. Zhou, C. Xhou, and Q. Li, *Space electronic reconnaissance: localization theories and methods*. John Wiley & Sons, 2014.

[7] G. Wang, Y. Li, and N. Ansari, “A semidefinite relaxation method for source localization using tdoa and fdoa measurements,” *IEEE Transactions on Vehicular Technology*, vol. 62, no. 2, pp. 853–862, 2012.

[8] K. Yang, L. Jiang, and Z.-Q. Luo, “Efficient semidefinite relaxation for robust geolocation of unknown emitter by a satellite cluster using tdoa and fdoa measurements,” in *2011 IEEE International Conference on Acoustics, Speech and Signal Processing (ICASSP)*. IEEE, 2011, pp. 2584–2587.

[9] L. Deng, P. Wei, Z. Zhang, and H. Zhang, “Doppler frequency shift based source localization in presence of sensor location errors,” *IEEE Access*, vol. 6, pp. 59 752–59 760, 2018.

[10] J. S. Picard and A. J. Weiss, “Time-delay and doppler-shift based geolocation by semi-definite programming,” in *2012 Proceedings of the 20th European Signal Processing Conference (EUSIPCO)*. IEEE, 2012, pp. 1189–1193.

[11] Y. S. Du, P. Wei, W. C. Li, and H. S. Liao, “Doppler shift based target localization using semidefinite relaxation,” *IEICE Transactions on Fundementals of Electronics, Communications and Computer Sciences*, vol. 97, no. 1, pp. 397–400, 2014.

[12] M. A. Nuhoğlu, A. Bayri, and H. A. Çırpan, “A novel doppler frequency geolocation method for multiple satellites,” in *IEEE Signal Processing and Applications Conference (SIU)*. IEEE, 2020 (Submitted).

[13] B. Lee, Y. Chan, F. Chan, H.-J. Du, and F. A. Dilkes, “Doppler frequency geolocation of uncooperative radars,” in *MILCOM 2007-IEEE Military Communications Conference*. IEEE, 2007, pp. 1–6.

[14] Z.-Q. Luo, W.-K. Ma, A. M.-C. So, Y. Ye, and S. Zhang, “Semidefinite relaxation of quadratic optimization problems,” *IEEE Signal Processing Magazine*, vol. 27, no. 3, pp. 20–34, 2010.

[15] L. Vandenberghe and S. Boyd, “Semidefinite programming,” *SIAM review*, vol. 38, no. 1, pp. 49–95, 1996.

[16] M. Grant and S. Boyd, “Cvx: Matlab software for disciplined convex programming, version 2.1,” 2014.

[17] K.-C. Toh, M. J. Todd, and R. H. Tütüncü, “Sdpt3-a matlab software package for semidefinite programming, version 1.3,” *Optimization methods and software*, vol. 1, no. 1-4, pp. 545–581, 1999.